

Supporting Information

High Surface Area Mesoporous Carbon Nanodendrites – Detonation Synthesis, Characterization and use as novel Electrocatalyst Support Material

Thomas Merzdorf ^{a,‡}, An Guo ^{a,‡}, Pierre Schröer ^a, Elisabeth Hornberger ^a, Sebastian Ott ^a,
Laurin Riebel ^a, Jessica Hübner ^a, Liang Liang ^a, Malte Klingenhof ^a, Matthias Kroschel ^a,
Marleen Hußmann ^b, Siegfried Eigler ^b, Alisa Kozhushner ^c, Lior Elbaz ^c, and Peter Strasser ^a

^a Department of Chemistry, Technische Universität Berlin, 10623 Berlin, Germany

^b Institut für Chemie und Biochemie, Freie Universität Berlin, 14195 Berlin, Germany

^c Chemistry Department, Bar-Ilan University, 5290002 Ramat-Gan, Israel

*Corresponding author: Peter Strasser, pstrasser@tu-berlin.de

‡ T.M. and A.G. contributed equally to this paper

T.M. and A.G. analyzed the data and composed the manuscript. S.O., A.G., P.Schr., L.R., A.K. and L.E. synthesized the MCND materials. A.G., E.H., L.R. performed the wet impregnation on the support materials, the XRD measurements and the RDE tests. M.Kr. performed the TGA measurement. The elemental analysis was performed by A.G., A.K. and L.E.. EM images were acquired by M.Kl. (TEM) and L.L. (SEM). J.H. and P.Schr. performed the physisorption experiments. M.H. and S.E. performed and analyzed the Raman spectroscopy. T.M. performed the MEA tests. P.St. supervised the study. All authors participated in the discussion.

Experimental Section.

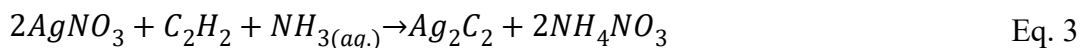
Synthesis of Mesoporous Carbon Nanodendrites.

For the mesoporous carbon nanodendrite (MCND) synthesis a multiple-step procedure was designed.¹ First of all, 2.55 g AgNO₃ (Alfa Aesar) was dissolved in 435 mL (40 mL 28% ammonium hydroxide ALFA AESAR + 395 mL water) aqueous ammonia solution. For silver acetylide (Ag₂C₂) formation the solution was bubbled with Ar for 15 min and a gas flow of 100 mL/min. Following this purging step, the gas flow was changed to acetylene (C₂H₂) at 50 mL/min and continuously sonicated. After 7 min sonification, the solution turned yellow/yellow-grey. The gas flow was kept constant with 1 min sonification every 3 min (to prevent any detonation of the product) for another 15 min. The final product was formed as a grey fluffy solid.

In aqueous solution, solved AgNO₃ reacts with acetylene (C₂H₂) gas to a very unstable Ag₂C₂ salt. Under non-alkaline conditions but solved in pure water an undesired conversion to Ag₂C₂ · AgNO₃ takes place (eq. 1) which then would decompose to metallic Ag and carbonoxid-gas (eq. 2). Thus, pure carbon wouldn't appear as a side product since it directly reacts with the oxygen groups from the silver complex.



To avoid the generation of such silver salts the reaction is conducted under sonification in an aqueous ammonia solution to buffer the created NO₃⁻ anion in form of ammonium-nitrate (eq. 3). Consequently, the reaction favors the generation of pure Ag₂C₂ which then will decompose to elemental silver and pure carbon (eq. 4).



Caution has to be taken handling this product. If dried out silver-acetylide is very sensitive to friction and heat and may detonate spontaneously with an explosive sound and shock wave. So, it has to be ensured that the product is kept wet at any point but can be filtered and washed with 300 mL methanol immediately. The grey matter was then placed in a Teflon beaker, put in a stainless-steel reactor, sealed tightly and set under vacuum (Figure S1). The reactor was placed in a heating mantel with a temperature control unit and equipped with two valves. One valve connecting the reactor with a vacuum pump having an overpressure valve in between and a second one to ventilate the inside of the reactor.

At the first heating step, the sample was heat up to 80 °C under vacuum overnight. This step enabled an encapsulation process of the silver-acetylide and dried the sample removing any liquid species such as water and methanol. In a second step, the sample was kept under vacuum and rapidly heated up to 220 °C. In the range from 170 – 210 °C a spontaneous detonation occurred, decomposing the silver-acetylide to dendritic-shaped carbon species covered with some solid Ag nanoparticles. The final powder was removed after cooling down the reactor naturally and ventilated with air. To remove any silver residues the black carbon powder was leached in 60 mL conc. HNO₃ for 1.5 h under continuous stirring and subsequently washed with 5 L hot water. After drying the washed carbon powder overnight in a vacuum oven, a final heat treatment was conducted in a tube furnace. Therefore, the sample was placed in a corundum boat and put in the oven. Under a constant Ar gas flow of 100 mL/min the oven was heated up to either 900, 1200 or 1500 °C with a heating ramp of 400 K/h and kept at the corresponding temperature for 12 hours before cooling down naturally. Thermogravimetric analysis (Figure S10) was performed using a STA 8000 (PerkinElmer, Inc.) under Ar atmosphere up to 1500 °C

(5 °C/min) to investigate the mass loss at high temperatures. The samples were placed in a corundum crucible and denominated in the manuscript according to their respective set temperatures (900, 1200 or 1500 °C).

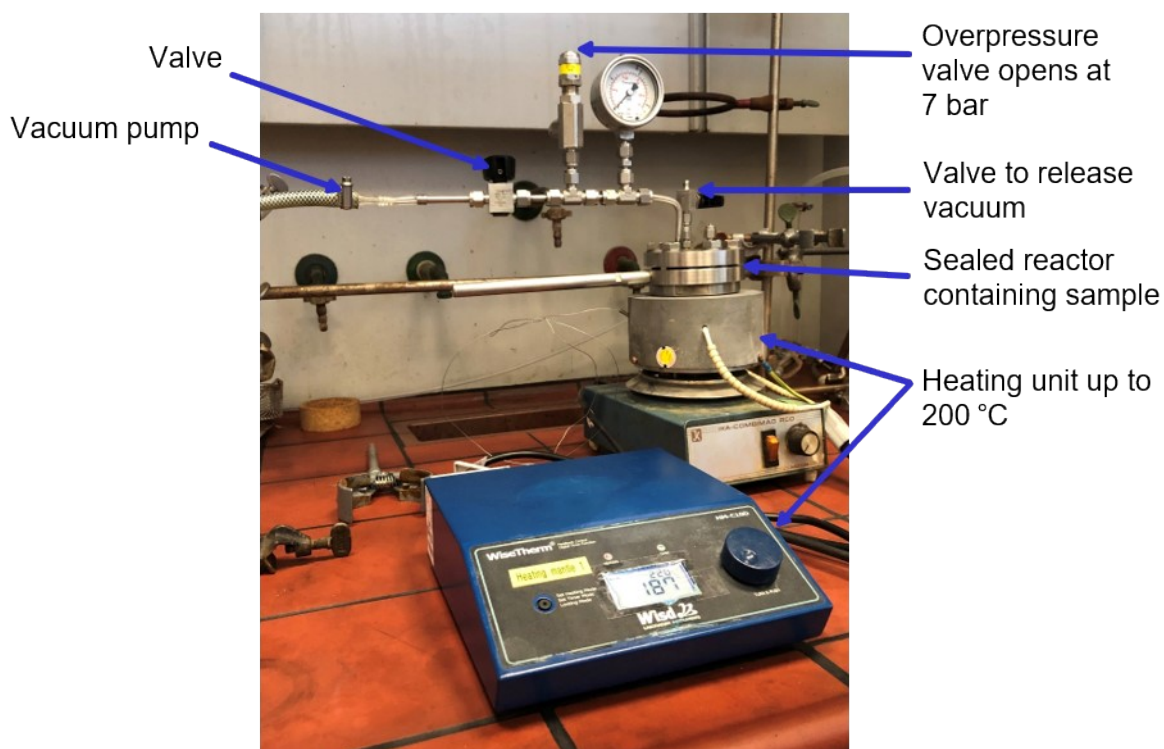


Figure S1: Setup of a stainless-steel reactor as controlled detonation place for Ag_2C_2 in a Teflon beaker. The figure shows the connection of the beaker (middle, right) to a temperature regulating unit (front) and a vacuum pump (left). Additionally, the reactor is equipped with two valves and one overpressure valve to regulate the pressure.

Pt Deposition on Carbon Supports.

Pt nanoparticles were deposited on the different carbon supports using a self-engineered fluidized bed reactor (FBR) following the procedure as described elsewhere.^{2, 3} 150 mg $\text{H}_2\text{PtCl}_6 \cdot 6\text{H}_2\text{O}$ were dissolved in 2 mL of a 1:1 mixture of ultrapure water and isopropanol. The Pt precursor was added to 200 mg carbon in 3 mL isopropanol to form a slurry and homogenized

within a cooling bath via a horn sonifier (Branson, output 6 W) for 15 min. The Pt-impregnated carbon was rapidly cooled in liquid N₂, dried in vacuum, and placed in the fluidized bed reduction reactor. The system was purged with N₂ to remove any air residues. Then, the atmosphere was switched to 4 % H₂ in Ar. The temperature was ramped at 5 K·min⁻¹ to 200 °C and held for 2 h. The atmosphere was switched back to N₂ and the system was allowed to naturally cool down to room temperature.

CHNS analysis.

The elemental compositions of the carbons (regarding C, H, N and S amounts) were determined with a Thermo FlashEA 1112 Organic Elemental Analyzer (Thermo Finnigan). An oxidizer (V₂O₅) was added for a dynamic flash combustion at 1020 °C in a manually stacked reactor (WO₃/Cu/Al₂O₃). Gas chromatography was used to identify and quantify the resulting gases.

Physisorption and Micropore Analysis.

The surface characteristics were determined using N₂ physisorption experiments. An Autosorb-1 (Quantachrome) instrument was used to acquire the isotherms at 77 K. The carbon powders were placed in a glass tube. For minimal dead volume, glass rods and glass wool were inserted on top of the carbon powder. For removal of any gas and water adsorbates, the samples were degassed for 24 h under vacuum at 80 °C. The adsorption and desorption isotherms were obtained for $10^{-6} \leq p/p_0 \leq 0.995$ (p : gas pressure, p_0 : saturation pressure). The overall surface area was determined using the multipoint Brunauer-Emmett-Teller (BET) method. The pore size distribution was analyzed employing a quenched solid density functional theory (QSDFT) model. The QSDFT model is based on the carbon adsorption branch kernel at 77 K and was

selected to match the pore morphology utilizing a slit pore model (pore diameter <2 nm) and cylindrical pore model (pore diameter >2 nm).

Electron Microscopy.

Scanning electron microscopy (SEM) was conducted to investigate the morphology of the carbon supports. SEM images were collected on a JEOL 7401F operated at 10 kV acceleration voltage.

Transmission Electron Microscopy (TEM) was performed to determine morphology of the Pt nanoparticles. TEM images were collected on a FEI Tecnai G² 20 S-TWIN equipped with a LaB₆ cathode operated at 200 kV acceleration voltage with 0.24 nm resolution limit. Stereoscopic TEM BrightField images were taken under specimen angles of 0 deg and +7 deg. StereoPhoto Maker V.4.22 was used to create anaglyph images and images for cross-view technique to get a quick 3-dimensional impression about the particle location.

Raman Spectroscopy.

Raman measurements were performed on XPLORA Plus (Horiba) with a horizontal polarized 532 nm Laser and an 100x objective (MPlan N, Olympus). Measurement conditions were set to 20 s acquisition time, two accumulations, 15 μ W laser power (0.1% filter), 1200 l/mm grating and slit and hole size of 200 μ m and 500 μ m, respectively. Each averaged Raman spectrum represents around 45 Raman data sets. Spectra of KB300 and Vulcan were baseline corrected within LabSpec 6. Data were analyzed with a Python script.

X-ray Diffraction.

X-ray diffraction patterns were conducted using a Bruker D8 advance powder diffractometer in Bragg–Brentano geometry with a Cu K α source. For minimum background signal, the samples

were placed on a Si plate. Data were collected in a 2θ range of 10° - 90° at a step size of 0.04° and $7\text{ s time}\cdot\text{step}^{-1}$.

Inductively Coupled Plasma Optical Emission Spectroscopy.

The Pt loadings were determined by inductively coupled plasma optical emission spectroscopy (ICP-OES) using a Varian 715-ES system with a CCD detector. After digestion in an acid solution of concentrated HNO_3 and HCl (1:3) using an Anton Paar multiwave GO microwave, the samples were diluted with ultrapure water, filtered and analyzed. Pt standard concentration of 1,2,7,10 and 12 ppm were used.

Rotating Disk Electrode.

The electrochemical performance of the catalysts was evaluated using a typical three-electrode setup with a working electrode (catalyst thin films drop casted on a glassy carbon rotating disk electrode, $A_{\text{geo}} = 0.196\text{ cm}^2$, Pt loading = $12.5\text{ }\mu\text{g}\cdot\text{cm}^2$), a counter electrode (Pt mesh) and a freshly calibrated reference electrode (mercury-mercury sulfate electrode) in 0.1 M HClO_4 electrolyte (perchloric acid, diluted with ultrapure water from 70 % HClO_4 , 99.998 5% trace metal bases, Sigma-Aldrich) connected with a BioLogic SP-200 potentiostat Catalyst inks consisted of $\sim 3\text{ mg}$ catalyst powder, 1.99 ml ultrapure water, 0.5 ml isopropanol and 0.01 ml 5 wt% Nafion solution. The potentials are iR -drop corrected stated against the RHE. The electrochemical protocol follows a typical routine as published elsewhere.³ The catalyst was conditioned for 50 cyclic voltammograms (CV) until a stable CV was recorded (0.05 - 1 V , $100\text{ mV}\cdot\text{s}^{-1}$, N_2 -saturated electrolyte). The Pt mass based (m_{Pt}) hydrogen under potential deposition electrochemical active surface area ($\text{ECSA}_{\text{H-upd}}$) was evaluated via charge integration of the hydrogen ad-/desorption region $Q_{\text{H-upd}}$ of the last cycle after double layer

current correction assuming a theoretical charge value Q_{theo} of $210 \mu\text{C}\cdot\text{cm}_{\text{Pt}}^{-2}$. The oxygen reduction reaction (ORR) activity was evaluated with linear sweep voltammetry (LSV, 0.05-1 V, 5mV s^{-1} , 1600 rpm, O_2 -saturated electrolyte). From the LSV curves, both diffusion-limited current and current at 0.9 V were extracted. The ORR activity was calculated following the Koutecký–Levich equation. The catalysts were tested regarding their Pt stability (10,000 square wave voltammograms (SWV) between 0.6 and 0.95 V with 3 s holding time at each potential) followed by $\text{ECSA}_{\text{H-upd}}$ and ORR activity evaluation after the stability test.

Fuel Cell Testing

Preparation and Assembly of Membrane Electrode Assembly (MEA)³

For the single cell fuel cell testing, an ink was produced with each of the six investigated catalysts, the ink was optimized to obtain a nicely dispersed solution. The solid fraction of the ink for the cathode catalyst was set to 0.5 wt%, with an I/C ratio of 0.6 in an isopropanol-water mixture with either 10 wt% or 80 wt% water, depending on the catalyst properties. This ink was then sonicated for 15 min with a horn sonifier. Using the EXACTACOAT spraycoater, the ink was sprayed onto the mesoporous side of a 10 cm² sized gas diffusion layer (GDL) (SIGRACET, 22BB) with a loading of 0.15 mg_{Pt}/cm². For the anode side, the ink consists of 1 wt% solid fraction with an I/C ratio of 0.6 and 10 wt% water using a 50 wt% Pt catalyst (Umicore). This ink was also sprayed onto the 22BB GDL with a loading of 0.1 mg_{Pt}/cm². An extra Nafion coating was sprayed on top of the GDLs with a 1 wt% Nafion solution. An anode and a cathode GDL were then hotpressed with the Nafion membrane (NR-212) at 146 °C for 4 minutes at 1.7 MPa_{abs}. The MEA was let cool down naturally and assembled in a 10 cm² single cell (FUEL CELL TECHNOLOGIES) with 10 Nm torque. The cathode gas exhaust of the fuel cell test stand (FUEL CELL TECHNOLOGIES) is connected to a nondispersive infrared analyzer (NDIR, SIEMENS) to obtain *online* gas concentrations of CO and CO₂ via infrared and O₂ with an oxygen sensor.

MEA Conditioning and Degradation Protocols

The MEA conditioning and the degradation protocols are already published elsewhere.³ The conditioning of the MEA consists of three potential holds at 0.6 V, OCP and 0.85 V for 45 min, 5 min and 10 min respectively at 80 °C and 100% RH repeated for 10 times. Afterwards, the MEA is characterized at 30% RH (85 °C) and 100% RH (80 °C), impedance measurements, CVs and polarization curves were measured with a potentiostat (HCP-803, BIOLOGIC) to determine the high frequency resistance (HFR), the cross-over current, the ECSA_{H-upd}, the mass activity and the proton resistance. The degradation protocol follows the suggested protocol of the US Department of Energy (DoE) for the support degradation with 5000 CVs between 1 and 1.5 V and 500 mV/s.⁴ During the degradation measurement, 8 different H₂/air polarization curves were measured always after 0, 10, 100, 200, 500, 1000, 2000 and 5000 CVs. Each polarization curve was conducted at 80 °C and 100% RH with 150 kPa backpressure, stoichiometry of 1.5 and 2 with minimal flows of 50 ml/min and 800 ml/min at the anode and cathode respectively. The minimal flow of 800 ml/min at the cathode was necessary to ensure accurate NDIR measurements. For each catalyst, at least two MEAs were prepared and tested to ensure reproducibility. The polarization curves were corrected for the cross-over current and the HFR of the cell and setup without catalyst layers.

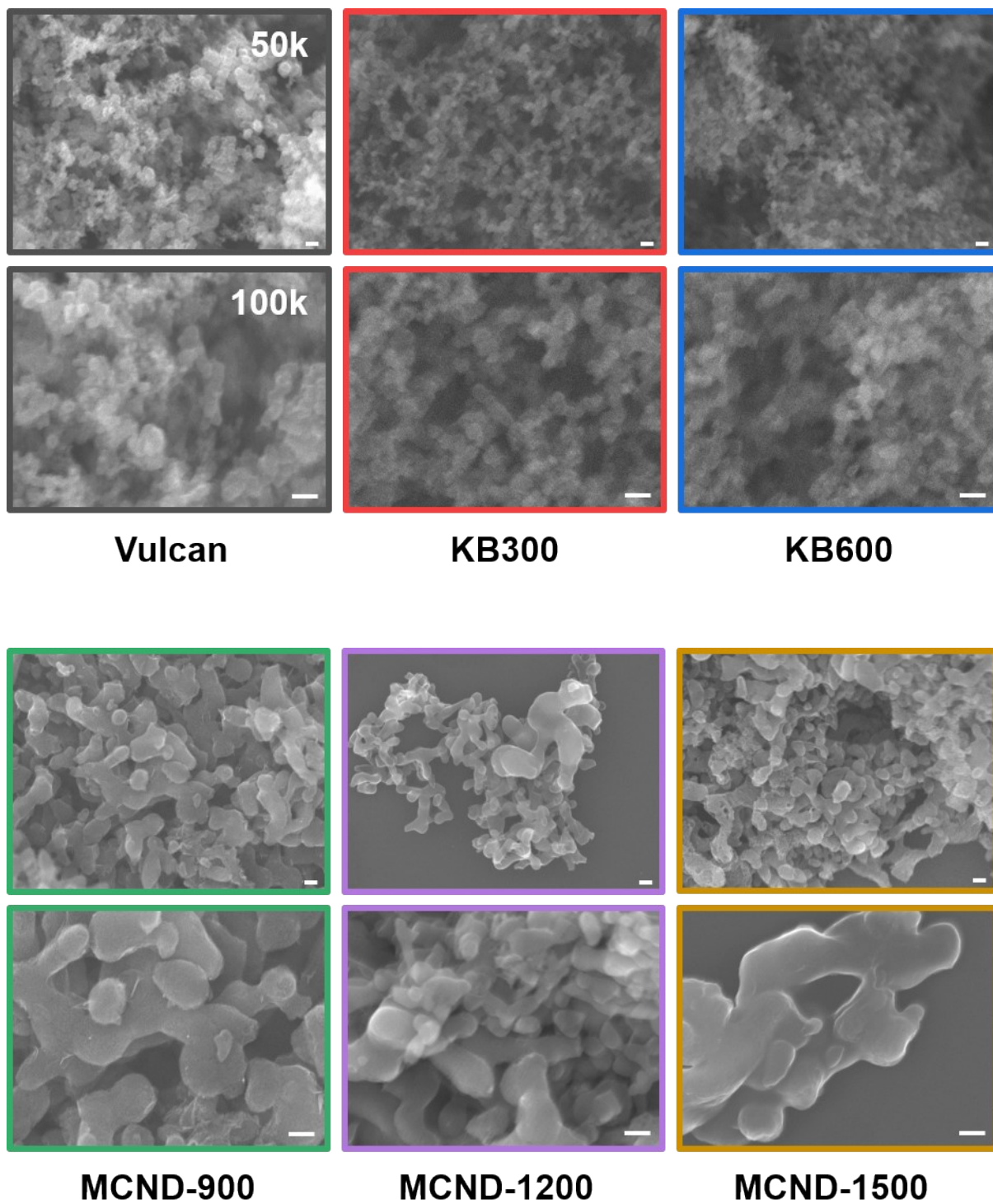


Figure S2. SEM images at 50k (top) and 100k (bottom) magnification of Vulcan (black), KB300 (red), KB600 (blue), MCND-900 (green), MCND-1200 (purple) and MCND-1500 (gold), the scale bar represents 100 nm.

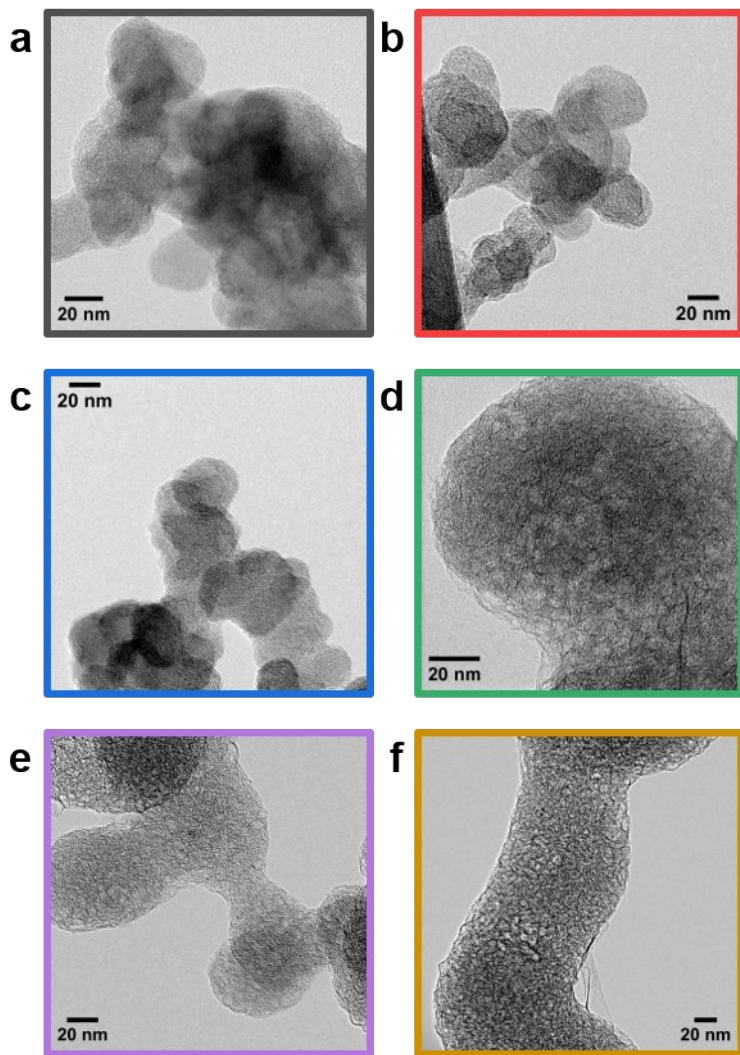


Figure S3: TEM images of a) Vulcan (black), b) KB300 (red), c) KB600 (blue), d) MCND-900 (green), e) MCND-1200 (purple), f) MCND-1500 (gold).

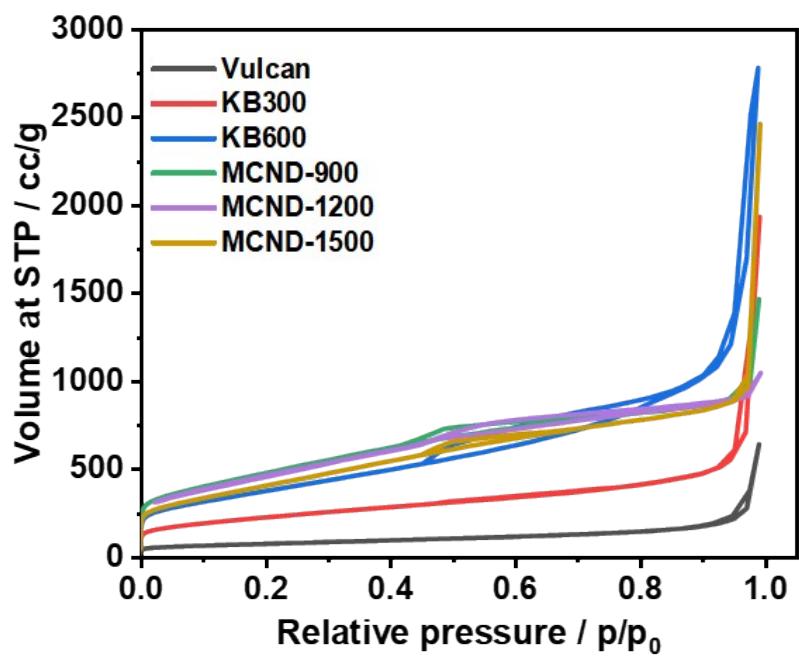


Figure S4. Results of physisorption. Isotherms of Vulcan (black), KB300 (red), KB600 (blue), MCND-900 (green), MCND-1200 (purple) and MCND-1500 (gold).

Table S1: Elemental composition and surface characteristics for MCND and commercial carbons. *Oxygen content calculated as difference to 100%.

Carbon material	% N	% C	% H	% S	*% O
Vulcan	0.00	98.10	0.00	0.00	1.90
KB300	0.00	98.87	0.02	0.00	1.11
KB600	0.00	98.43	0.19	0.00	1.38
MCND-900	0.04	97.20	0.00	0.00	2.76
MCND-1200	0.00	97.59	0.00	0.00	2.41
MCND-1500	0.00	97.70	0.00	0.00	2.30

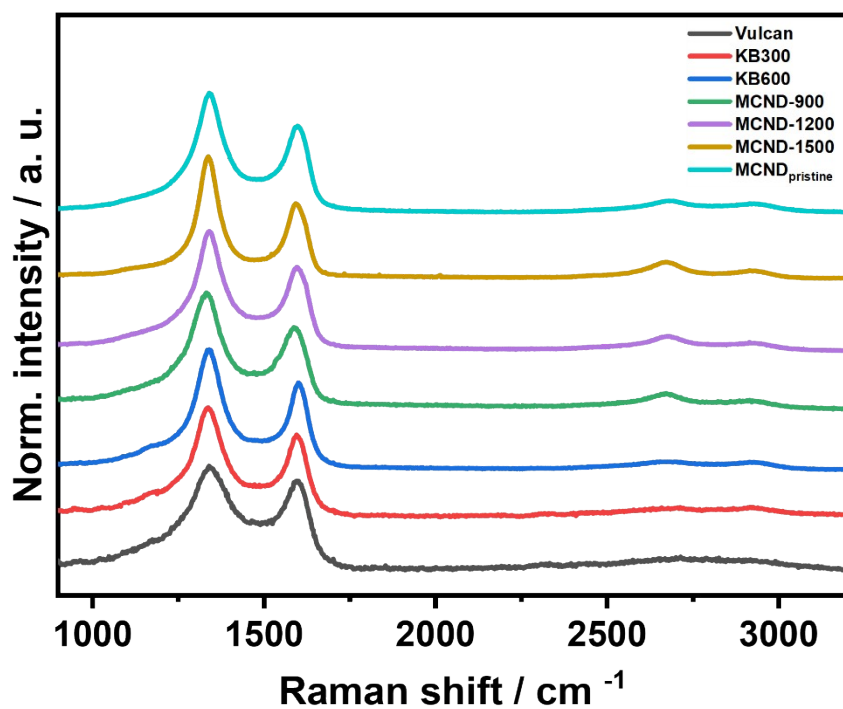


Figure S5. Average Raman spectra of Vulcan (black), KB300 (red), KB600 (blue), MCND-900 (green), MCND-1200 (purple), MCND-1500 (gold) and MCND_{pristine} (unannealed, turquoise) with normalized intensity stacked with offset.

Table S2. Evolution of the electrochemical parameters in terms of ECSA, ORR mass activity and specific activity for Pt/Vulcan, Pt/KB300, Pt/KB600, Pt/MCND-900, Pt/MCND-1200 and Pt/MCND-1500 determined using RDE experiments.

Details	Pt loading / wt-%	ECSA- H_{upd}	ECSA- H_{upd}	$MA_{0.9\text{V}}$	$MA_{0.9\text{V}}$	SA	SA
		BOL / $\text{m}^2 \text{g}_{\text{Pt}}^{-1}$	EOL / $\text{m}^2 \text{g}_{\text{Pt}}^{-1}$	BOL / $\text{A mg}_{\text{Pt}}^{-1}$	EOL / $\text{A mg}_{\text{Pt}}^{-1}$	BOL / mA cm^{-2}	EOL / mA cm^{-2}
Pt/Vulcan	21.1	70 ± 8	59 ± 5	0.33 ± 0.06	0.31 ± 0.10	0.71 ± 0.25	0.50 ± 0.12
Pt/KB300	20.8	132 ± 2	103 ± 2	0.43 ± 0.07	0.53 ± 0.09	0.33 ± 0.05	0.51 ± 0.09
Pt/KB600	18.7	131 ± 19	90 ± 18	0.35 ± 0.01	0.29 ± 0.07	0.27 ± 0.03	0.32 ± 0.01
Pt/MCND-900	24.1	107 ± 3	91 ± 5	0.31 ± 0.05	0.36 ± 0.06	0.29 ± 0.04	0.40 ± 0.06
Pt/MCND-1200	26.2	73 ± 6	54 ± 3	0.12 ± 0.02	0.16 ± 0.04	0.17 ± 0.02	0.29 ± 0.07
Pt/MCND-1500	20.5	122 ± 7	77 ± 9	0.20 ± 0.03	0.27 ± 0.08	0.16 ± 0.06	0.35 ± 0.10

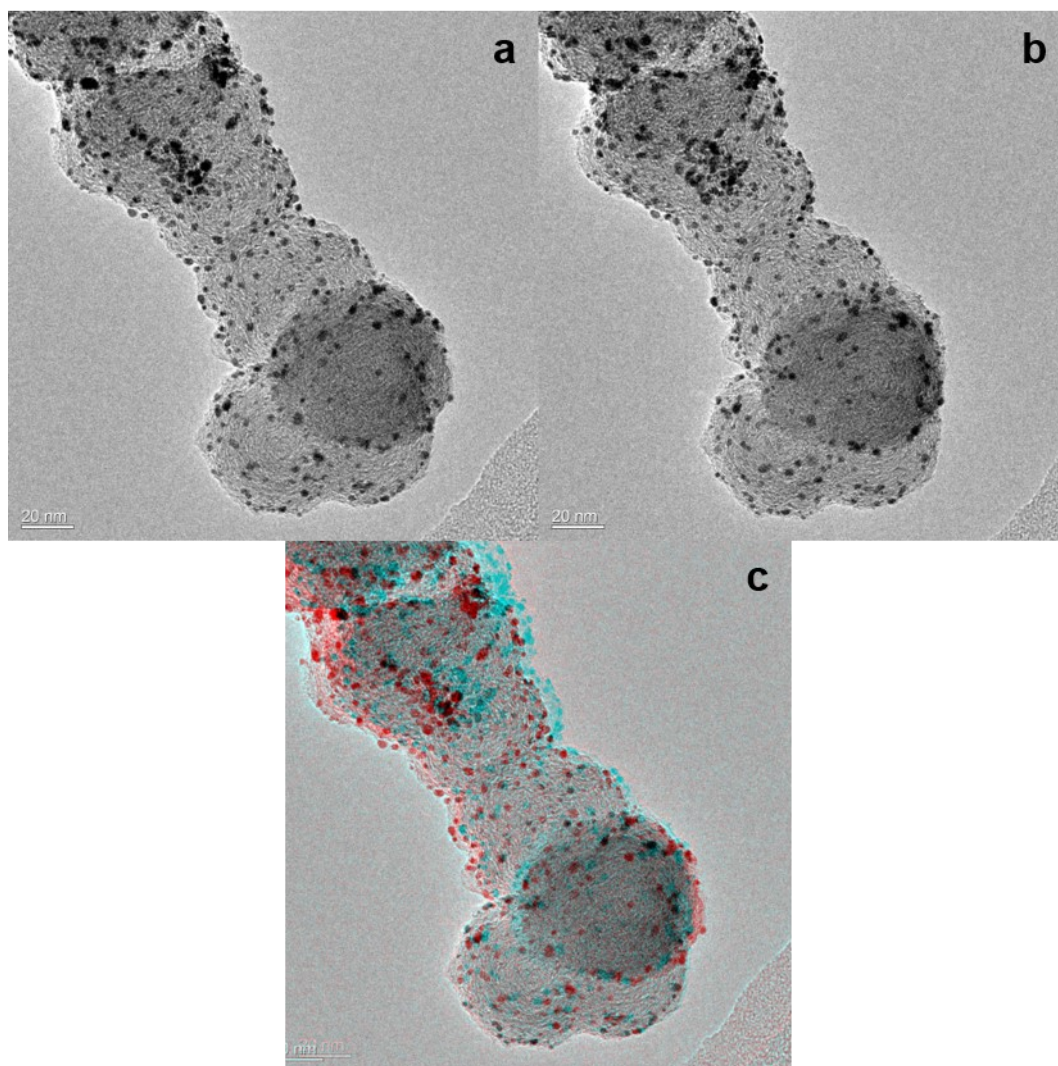


Figure S6: Stereoscopic TEM images of Pt/Vulcan showing Pt nanoparticles placed on the outside of the carbon particles, the scale bar represents 20 nm; a,b) TEM images for cross-view with specimen angle of 0 deg. (a) and +7 deg. (b); c) anaglyph image of both images.

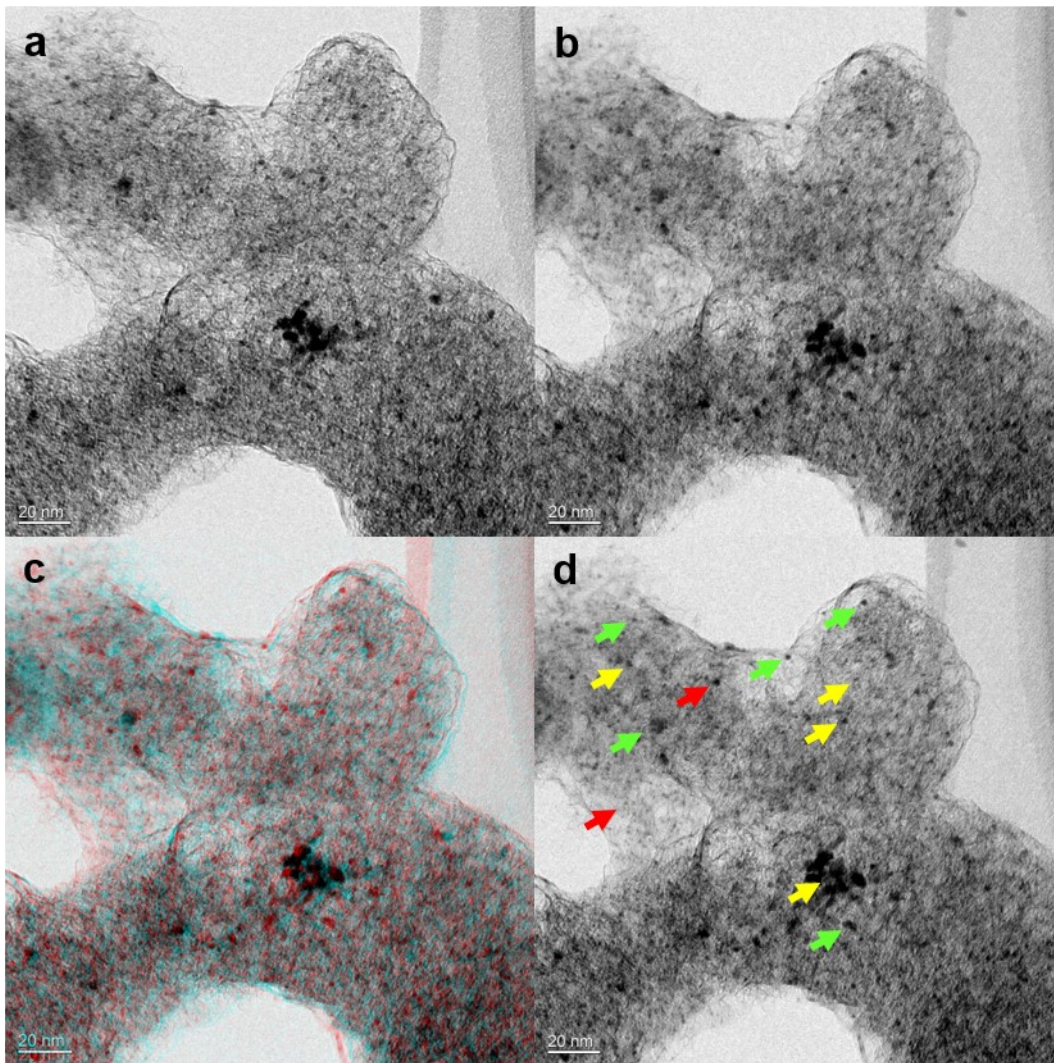


Figure S7: Stereoscopic TEM images of Pt/MCND-1500 showing Pt nanoparticles placed in pores and on the outside of the carbon particles, the scale bar represents 20 nm; a,b) TEM images for cross-view with specimen angle of 0 deg. (a) and +7 deg. (b); c) anaglyph image of both images. d) particles marked on top of carbon (green), on the back (red) and inside pores (yellow).

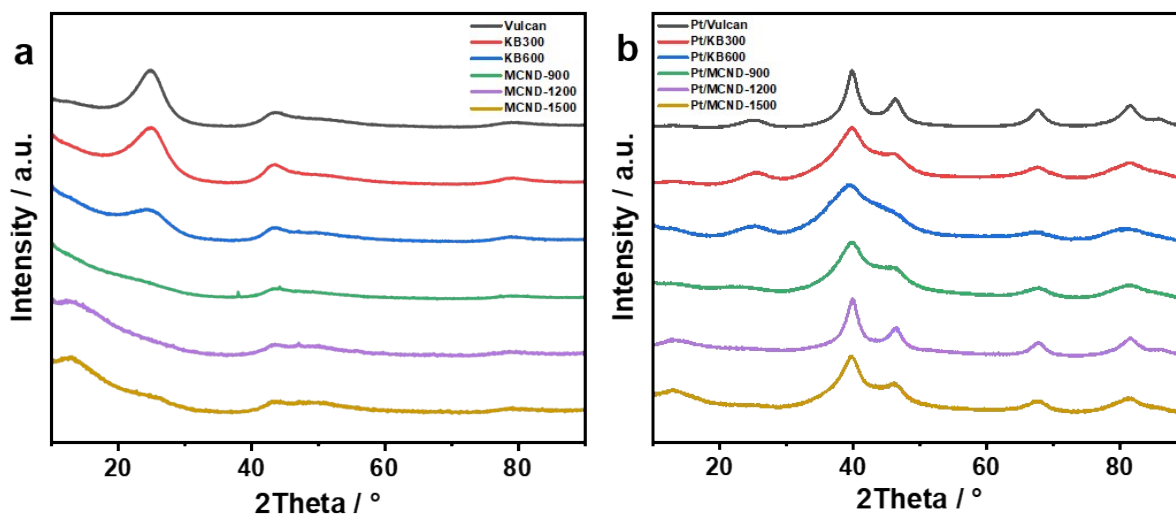


Figure S8. XRD patterns of a) pure carbons for Vulcan (black), KB300 (red), KB600 (blue), MCND-900 (green), MCND-1200 (purple) and MCND-1500 (gold) and b) their platinumized version.

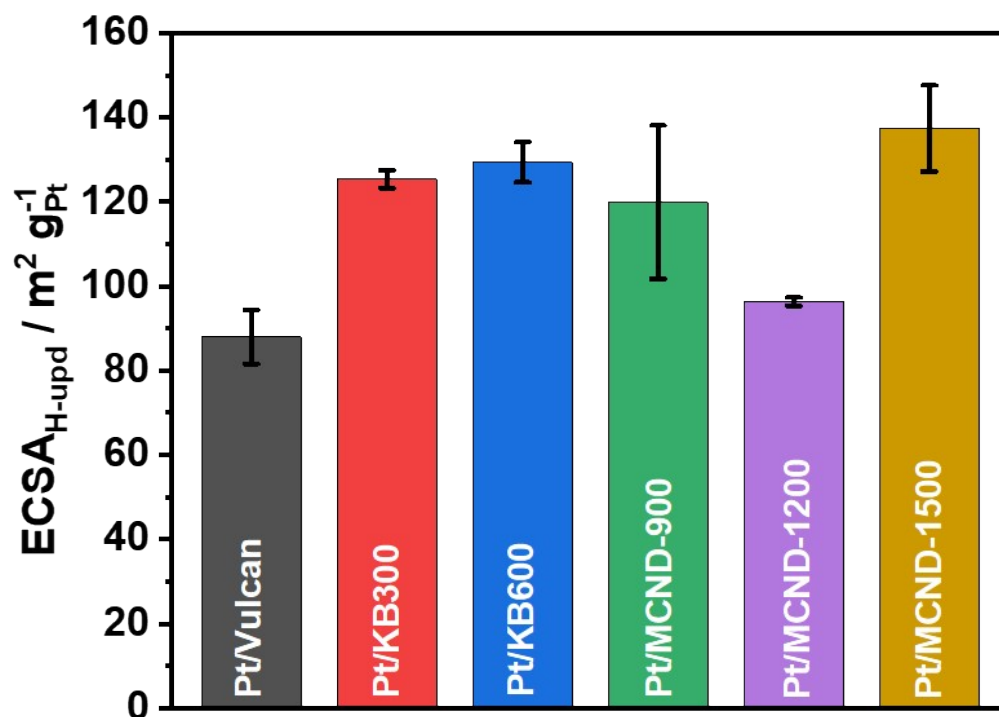


Figure S9: ECSA measured in MEA at BOL for Pt/Vulcan (black), Pt/KB300 (red), Pt/KB600 (blue), Pt/MCND-900 (green), Pt/MCND-1200 (purple) and Pt/MCND-1500 (gold).

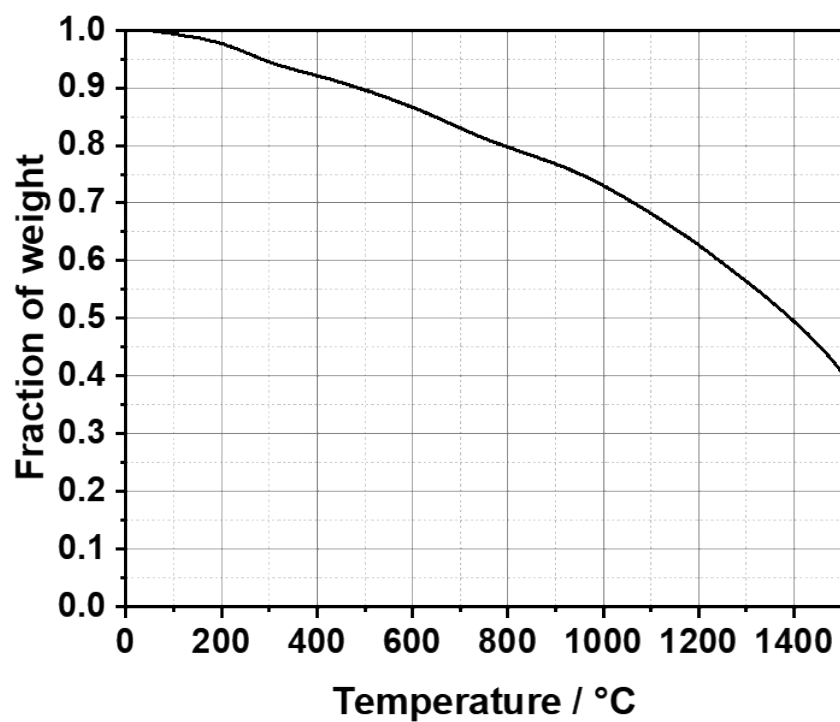


Figure S10: Thermogravimetric analysis (TGA) of pristine MCND (unannealed) under Ar atmosphere, ramping to 1500 °C with 5 K/min.

References:

- (1) Numao, S.; Judai, K.; Nishijo, J.; Mizuuchi, K.; Nishi, N. Synthesis and characterization of mesoporous carbon nano-dendrites with graphitic ultra-thin walls and their application to supercapacitor electrodes. *Carbon* **2009**, *47* (1), 306-312. DOI: 10.1016/j.carbon.2008.10.012.
- (2) Hornberger, E.; Schmies, H.; Paul, B.; Kühl, S.; Strasser, P. Design and Validation of a Fluidized Bed Catalyst Reduction Reactor for the Synthesis of Well-Dispersed Nanoparticle Ensembles. *J. Electrochem. Soc.* **2020**, *167* (11), 114509. DOI: 10.1149/1945-7111/aba4eb.
- (3) Hornberger, E.; Merzdorf, T.; Schmies, H.; Hubner, J.; Klingenhof, M.; Gernert, U.; Kroschel, M.; Anke, B.; Lerch, M.; Schmidt, J.; et al. Impact of Carbon N-Doping and Pyridinic-N Content on the Fuel Cell Performance and Durability of Carbon-Supported Pt Nanoparticle Catalysts. *ACS Appl Mater Interfaces* **2022**, *14* (16), 18420-18430. DOI: 10.1021/acsami.2c00762.
- (4) Energy, U. S. D. o. *Multi-Year Research, Development, and Demonstration Plan - Section 3.4 Fuel Cells*. U.S. Department of Energy, 2018. (accessed 09.03.2024).